1 mJ pulse bursts from a Yb-doped fiber amplifier

H. Kalaycıoğlu,[1,*] Y. B. Eldeniz,[2] Ö. Akçaalan,[1] S. Yavaş,[1] K. Gürel,[1] M. Efe,[2] and F. Ö. Ilday[1]

[1]*Department of Physics, Bilkent University, Cankaya, Ankara 06800, Turkey*

[2]*Department of Electronics Engineering, Ankara University, Tandogan, Ankara 06100, Turkey*

**Corresponding author: hamitkal@bilkent.edu.tr*

Received March 6, 2012; revised May 1, 2012; accepted May 6, 2012;
posted May 7, 2012 (Doc. ID 164289); published June 22, 2012

We demonstrate burst-mode operation of a polarization-maintaining Yb-doped fiber amplifier capable of generating 60 μJ pulses within bursts of 11 pulses with extremely uniform energy distribution facilitated by a novel feedback mechanism shaping the seed of the burst-mode amplifier. The burst energy can be scaled up to 1 mJ, comprising 25 pulses with 40 μJ average individual energy. The amplifier is synchronously pulse pumped to minimize amplified spontaneous emission between the bursts. Pulse propagation is entirely in fiber and fiber-integrated components until the grating compressor, which allows for highly robust operation. The burst repetition rate is set to 1 kHz and spacing between individual pulses is 10 ns. The 40 μJ pulses are externally compressible to a full width at half-maximum of 600 fs. However, due to the substantial pedestal of the compressed pulses, the effective pulse duration is longer, estimated to be 1.2 ps. © 2012 Optical Society of America

OCIS codes: 060.2310, 060.2320, 140.3425, 270.2500.

There is much interest in fiber amplification of ultrashort pulses, which offers practical advantages, such as low cost, highly robust operation, and high-gain amplification [1,2]. These aspects are particularly important for industrial material processing, where fiber lasers are poised to make a significant impact.

The majority of ultrafast laser systems generate pulse trains consisting of nominally identical pulses, which are equally spaced in time. There is an interesting alternative, where the laser amplifier produces a group or burst of a limited number of high-repetition-rate pulses, and this burst itself is repeated at a much lower repetition rate [3–11]. In addition to several niche applications, including laser systems in accelerators [7,8], combustion diagnostics [9], flow measurements in aerodynamics [10], Thomson scattering experiments [11], and photoacoustic microscopy [12], this mode of operation possess great potential for ultrafast material processing [3,5,6,13], where a burst of closely spaced pulses can have an effect similar to that of a single pulse of energy equal to that of the entire burst [5]. In [6], the authors report sixfold increase in material ablation rates when six lower-energy pulses separated by 20 ns are used compared to a single pulse with energy equal to the sum of the burst. Similar results can be expected in tissue processing. In addition, burst-mode operation allows an additional degree of freedom to optimize material ablation while keeping thermal effects minimized. Thermal effects depend predominantly on the average power used, while material ablation depends on the peak power. Strength of the thermal effects can be controlled through the burst repetition rate, while ablation efficiency can be kept high through the use of high-repetition-rate and high-energy pulses within the burst. To date, burst-mode laser systems have relied on solid state lasers. Recently, we demonstrated the first high-energy, synchronously pulsed-pumped, burst-mode fiber laser [4] with 20 μJ per pulse and 250 μJ per burst. However, gain within the burst could not be fully controlled, resulting in large variations in pulse energy.

Here, we report on the use of an advanced preshaping method, which allows us to achieve less than 2% variation in pulse energy within the burst, limited by noise in the detection electronics, while at the same time scaling up the individual pulse energy to 60 μJ and the burst energy to 660 μJ at 1 kHz. We further demonstrate the possibility of generating bursts with total energies of 1 mJ, limited by available peak pump power, comprising 25 pulses each with 40 μJ average energy and <7% variation in pulse energy. These pulses are externally compressed to an effective pulse width of 1.2 ps.

The experimental setup (Fig. 1) consists of an all-normal dispersion laser oscillator [14], seeding three stages of core-pumped fiber preamplifiers and a double-clad fiber power amplifier, as well as synchronized pulse picking and pulsed-pumping electronics. Details of the setup not provided here can be found in [4,15]. The fiber oscillator operates at a repetition rate of 100 MHz and outputs 85 mW, centered at 1035 nm. The oscillator output is polarized with an in-line polarization beam splitter, followed by polarization-maintaining (PM) components. The seed pulses, with a bandwidth of 19 nm, are stretched to 360 ps in a 450-m-long PM fiber. The signal is amplified to about 600 mW by two stages of preamplifiers, which are pumped continuously at 976 nm, each with 450 mW. This is followed by a fiber-integrated acousto-optic modulator (AOM), which impresses the desired pulse burst mode. The AOM has 2.3 dB insertion

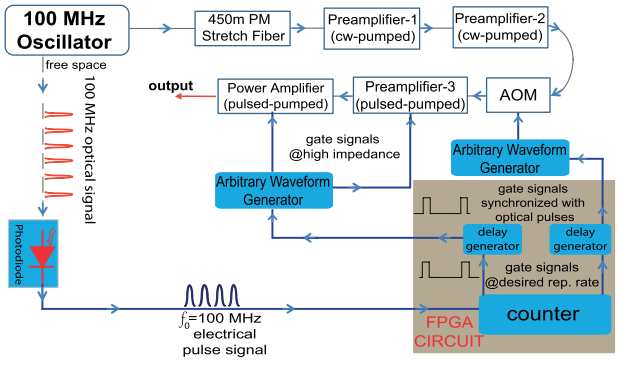

Fig. 1. (Color online) Schematic diagram of the experimental setup.

loss, 50 dB extinction, and rise and fall times of 6 and 8 ns, respectively. The bursts are amplified in the third preamplifier and thereafter the power amplifier, which are both pumped by pulsed sources in synchrony with the signal burst. Two arbitrary waveform generators (AWGs) and a field programmable gated array (FPGA) circuit are used to drive the AOM and the pulsed pump diodes. The FPGA circuit is triggered by the oscillator signal and, in turn, it triggers the AWGs that drive the AOM and the pump diodes. In this way, phase locking of the pump drive signals and the AOM gate signal to the seed signal minimizes the jitter of the pulses inside the burst and facilitates the homogenization of the energy distribution within the burst. For the power amplifier, backward pumping delivered through bulk optics is utilized and the gain fiber is kept short to help minimize the effective nonlinearity and keep the gain peak around 1030 nm.

During high-energy operation, depletion of the gain during the burst becomes considerable, leading to significant variation in pulse energy across the burst. The variation across the burst can be partially offset by modulating the input burst signal through the AOM such that the net gain times the launched pulse energy is nearly constant. Further homogenization of the individual pulse energy inside the burst is possible by optimizing the ramp signal applied to the AOM. It is evident that, by impressing a complex variation on the launched burst, one can obtain an arbitrarily uniform amplified pulse train at the cost of decreased efficiency, the extent of which increases for longer burst duration. To this end, we have developed an optimization algorithm to obtain a systematic method of pulse-energy homogenization for a burst of arbitrary duration. The algorithm starts by assigning a trial ramp signal, then, based on the resulting amplified burst, the transmittance values through the AOM are finely adjusted for individual pulses, starting from the last pulse and scanning until the earliest pulse. Next, the standard variation is calculated for the burst shape obtained. This procedure is repeated a number of times until no appreciable improvement in the standard deviation is obtained. We present the amplified pulse train for a modest 150 μJ burst with no precompensation in Fig. 2(a) to illustrate the importance of precompensation. Using the precompensation algorithm, we obtain our highest energy per pulse of 60 μJ for a burst duration of 660 ns, which contains 11 pulses [Fig. 2(b)]. The measured standard deviation with respect to the mean pulse energy is $<2\%$, a remarkable improvement compared to 116% for the uncompensated case [Fig. 2(a)] with much lower energy. The total burst energy is 660 μJ and the average output power is 660 mW. This corresponds to a pump-to-signal conversion of 48% with respect to coupled pump power and the net gain of 28 dB for the final stage amplifier. The amplified spontaneous emission (ASE) content in the final output is estimated to be about 2.5% based on simulations and experimentally confirmed to be definitely below an upper limit of 10%, obtained by applying the same pump power with no signal.

In order to extract even higher burst energy from the system and test the limits of our system, the burst duration has to be increased. This is because the system is currently limited by available pump energy, in terms of peak pump power physically and in terms of pump pulse duration to limit ASE formation, and the preamplifier stages are also operated close to their limits. Increasing the number of pulses within the burst, hence the burst duration to 250 ns, we obtain 775 mW, corresponding to 775 μJ of burst energy at 1 kHz. As for preshaping to homogenize the pulse energy inside the burst, it becomes increasingly difficult for longer bursts containing larger number of pulses and the cost, paid in terms of decreased efficiency, increases significantly. Nevertheless, we still obtain a high degree of uniformity of $<5\%$ [Fig. 2(c)]. Finally, we push for maximum burst energy, while keeping acceptably uniform pulse energy. We obtain 1 W output power, corresponding to an amplified burst energy of 1 mJ at 1 kHz, with 40 μJ individual pulse energy with 25 pulses in each burst [Fig. 2(d)]. The pump-to-signal conversion is 50% and the signal gain is 30 dB. As a result of a compromise between total burst energy and uniform distribution of pulse energy, the pulse train in Fig. 2(b) reflects a $<7\%$ homogenization level. Further increases in burst energy would result in sharply increased pulse-energy variation within the burst. It seems, however, possible to increase the burst energy at fixed burst duration by employing higher peak power pumping.

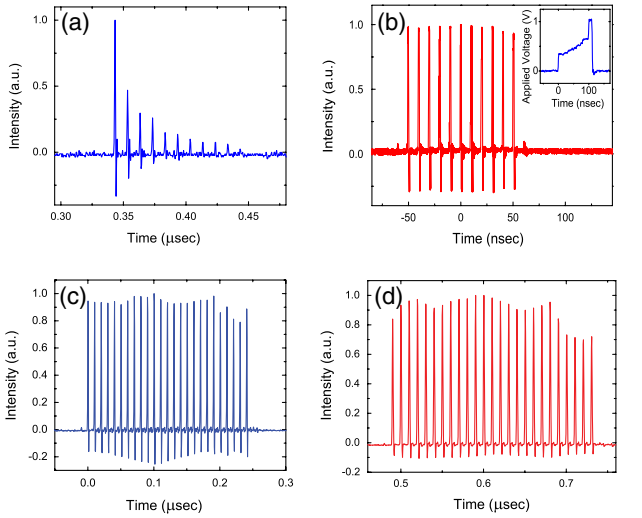

Fig. 2. (Color online) Temporal profile of the amplified burst with total energy of (a) 150 μJ, with no precompensation; (b) 660 μJ, comprised of 11 60 μJ pulses (pulse-energy variation of $<2\%$); (c) 775 μJ, comprised of 25 31 μJ pulses (pulse-energy variation of $<5\%$); and (d) 1 mJ, comprised of 25 40 μJ pulses (pulse-energy variation of $<7\%$). Inset to (b), corresponding AOM gate signal.

The amplifier, with its large nonlinear phase shift and third-order dispersion (TOD) mismatch, operates deep in the nonlinear chirped-pulse amplification regime [16,17] and the nonlinear phase shift for the power amplifier at 40 μJ pulse energy is estimated to be 16π through numerical simulations based on the method described in [18]. The highly uniform 40 μJ pulses with 1 mJ total burst energy are compressed in an external grating compressor. The autocorrelation result in Fig. 3(b) shows the presence of a significant pedestal due to residual TOD and self-phase modulation. The effective pulse duration is estimated to be 1.2 ps, based on an inferred pulse

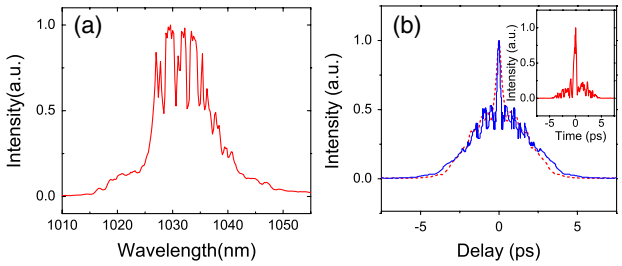

Fig. 3. (Color online) (a) Measured optical spectrum of the burst-mode amplifier output with 40 μJ energy per pulse and total of 1 mJ energy per burst. (b) Measured (blue solid curve) and retrieved (red dashed curve) autocorrelation of the dechirped pulses at the same energy level. Inset: retrieved pulse shape using the PICASO algorithm based on the autocorrelation and spectrum measurements.

shape, retrieved using the PICASO algorithm [19] and the autocorrelation and optical spectrum measurements.

In conclusion, we report on record-high individual pulse energy of 60 μJ within bursts of 660 μJ total energy, as well as record-high pulse-energy extraction of 1 mJ per burst from a synchronously pumped Yb-doped fiber amplifier. To the best of our knowledge, these pulse energy and pulse-energy extraction results represent record highs. The individual pulse-energy level is sufficiently high for a large range of likely applications, ranging from material processing to use as photoinjector lasers in accelerator facilities to lidar systems. We demonstrate the successful implementation of a novel feedback mechanism based on the amplifier output and acting on the AOM used for preshaping the burst pulse train to obtain extremely uniform pulse energy (variations of $<2\%$ in pulse energy within the burst, limited by the detection electronics). Given the relative simplicity of the amplifier, including its nearly all-fiber-integrated design, and its reliance on standard, off-the-shelf fibers, we believe that it is an attractive alternative to solid state lasers for material processing. The latter systems routinely produce 1 mJ and higher pulse energies and traditional fiber lasers are limited to a few tens of microjoules in energy, which limits their application. It has been argued theoretically and demonstrated experimentally that bursts of pulses behave practically like a single pulse in material processing when the pulse-to-pulse separation is 10 ns or less [5]. Consequently, the present system might offer the performance comparable to a 1 mJ laser system in material processing, with many practical advantages due to its reliance on fiber technology.

This work was supported by the European Union (EU) FP7 CROSS TRAP (Grant No. 244068) and the SANTEZ Project (No. 00255.STZ.2008-1).

References

1. D. J. Richardson, J. Nilsson, and W. A. Clarkson, J. Opt. Soc. Am. B **27**, B63 (2010).
2. J. Nilsson and D. N. Payne, Science **332**, 921 (2011).
3. M. Lapczyna, K. P. Chen, P. R. Herman, H. W. Tan, and R. S. Marjoribanks, Appl. Phys. A **69**, S883 (1999).
4. H. Kalaycioglu, K. Eken, and F. Ö Ilday, Opt. Lett. **36**, 3383 (2011).
5. W. Hu, Y. C. Shin, and G. King, Appl. Phys. A **98**, 407 (2010).
6. R. Knappe, H. Haloui, A. Seifert, A. Weis, and A. Nebel, Proc. SPIE **7585**, 75850H (2010).
7. H. Braun, R. Corsini, J. Delahaye, A. de Roeck, S. Döebert, A. Ferrari, G. Geschonke, A. Grudiev, C. Hauviller, B. Jeanneret, E. Jensen, T. Lefevre, Y. Papaphilippou, G. Riddone, L. Rinolfi, W. D. Schlatter, H. Schmickler, D. Schulte, I. Syratchev, M. Taborelli, F. Tecker, R. Toms, S. Weisz, and W. Wuensch, "CLIC 2008 Parameters," CERN-OPEN-2008-021 (European Organization for Nuclear Research, 2008).
8. I. Will, H. I. Templin, S. Schreiber, and W. Sandner, Opt. Express **19**, 23770 (2011).
9. P. Wu, W. R. Lempert, and R. B. Miles, AIAA J. **38**, 672 (2000).
10. B. S. Thurow, A. Satija, and K. Lynch, Appl. Opt. **48**, 2086 (2009).
11. D. J. Hartog Den, J. R. Ambuel, M. T. Borchardt, A. F. Falkowski, W. S. Harris, D. J. Holly, E. Parke, J. A. Reusch, P. E. Robl, H. D. Stephens, and Y. M. Yang, Rev. Sci. Instrum. **81**, 10D513 (2010).
12. T. Liu, J. Wang, G. I. Petrov, V. V. Yakovlev, and H. F. Zhang, Med. Phys. **37**, 1518 (2010).
13. M. Murakami, B. Liu, Z. Hu, Z. Liu, Y. Uehara, and Y. Che, Appl. Phys. Express **2**, 042501 (2009).
14. A. Chong, J. Buckley, W. Renninger, and F. W. Wise, Opt. Express **14**, 10095 (2006).
15. P. K. Mukhopadhyay, K. Özgören, I. L. Budunoğlu, and F. Ö. Ilday, IEEE J. Sel. Top. Quantum Electron. **15**, 145 (2009).
16. S. Zhou, L. Kuznetsova, A. Chong, and F. W. Wise, Opt. Express **13**, 4869 (2005).
17. H. Kalaycioglu, B. Oktem, C. Senel, P. P. Paltani, and F. Ö. Ilday, Opt. Lett. **35**, 959 (2010).
18. B. Oktem, C. Ülgüdür, and F. Ö. Ilday, Nat. Photon. **4**, 307 (2010).
19. J. W. Nicholson, J. Jasapara, W. Rudolph, F. G. Omenetto, and A. J. Taylor, Opt. Lett. **24**, 1774 (1999).